R. DEVI, B. POTUKUCHI
Department of Physics, University of Jammu
(Jammu Tawi-180006, India; e-mail: rituhans4028@gmail.com)

PION PRODUCTION IN ν_μ CHARGED CURRENT INTERACTIONS ON ^{40}Ar IN DEEP UNDERGROUND NEUTRINO EXPERIMENT

UDC 539

Understanding the pion generation and the consequences of final-state interactions (FSI) are critical for the data processing in all neutrino experiments. The energy utilized in modern neutrino researches of the resonance (RES) generation processes contributes significantly to the pion production. If a pion is absorbed in the nuclear matter after its production, the event may become unrecognizable from a quasielastic (QE) scattering process and act as a background. For oscillation experiments, estimating this background is critical, and it necessitates solid theoretical models for both pion generation at the primary vertex and after FSI. The number of pions created after FSI differs greatly from the number produced at the primary vertex due to FSI. Because neutrino detectors can only detect final-state particles, FSI obscures the proper information about particles created at the primary vertex. A detailed study of FSI is required to overcome this problem, which theoretical models incorporated in Monte Carlo (MC) neutrino event generators can provide. They should give theoretical results concerning the neutrino interactions for various researches, acting as a connection among both theoretical models and experimental data. In this paper, we provide simulated events for the pion creation in ν_μ charge current (CC) interactions on a ^{40}Ar target in the Deep Underground Neutrino Experiment (DUNE) setup for two distinct MC generators: GENIE and NuWro. In comparison to GENIE (v-3.00.06), NuWro (v-19.02.2) is more opaque (less responsive) to the charge exchange and absorption processes; pions are more likely to be absorbed than produced during the intranuclear transport.

K e y w o r d s: final-state interactions, cross-section, neutrino-nucleon scattering, primary hadronic system.

1. Introduction

Neutrino physics is reaching a precise era, powered by new experiments and contemporary detector technology, and this necessitates a better theoretical and phenomenological explanations of neutrino interactions. Neutrinos rarely interact with matter and can move rapidly without interaction with it. The properties of neutrinos are yet unknown, making their study difficult from both theoretical and experimental standpoints. The neutrino interactions are described by the Standard Model (SM)'s electroweak theory. SM assumed the neutrino was a massless particle in its previous formulation. Hence, the mass mixing was not expected, unlike quarks. If neutrinos had mass, the mass mixing would be possible in the lepton sector, and a neutrino generated in one flavor could later be seen as a neutrino of some other flavor, a phenomenon known as neutrino oscillations. The masslessness of neutrinos is not required by any fundamental physics principle. The Pontecorvo–Maki–Nakagawa–Sakata (PMNS) matrix [1] defines the strength of mass mixing in the leptonic sector. Three mixing angles ($\theta_{12}, \theta_{23}, \theta_{13}$), and the CP phase factor ($\delta_{\rm CP}$) can be used to represent PMNS. Apart from these mass

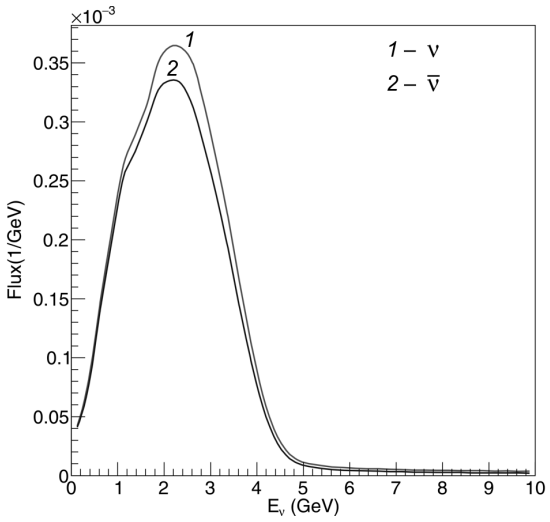

Fig. 1. The DUNE flux as a function of the neutrino energy used in our work

mixing factors, the probability of the neutrino oscillation is determined by the mass of neutrinos (or the difference of their squares), i.e., $\Delta m^2_{21} = m^2_2 - m^2_1$; $\Delta m^2_{32} = m^2_3 - m^2_2$; $\Delta m^2_{31} = m^2_{32} + m^2_{21}$.

Understanding the CC neutrino-nucleus interactions in the few GeV energy region is critical for current and future neutrino experiments. However, understanding the neutrino-nucleus cross-sections, the modelling of hadronization and intranuclear hadron transport, the description of nuclear models and nuclear effects in this energy region is difficult and requires many intermediate steps. For this, we will need a conventional MC generator that can account for all of these phases. GENIE [2], ANIS [3], NuWro [4], GiBUU [5], MARLEY [6], NEUT [7], and Nuance [8] are some of the MC generators devoted to the modeling of neutrino interactions. All of these generators have the same assumptions. Each generator considers primary and final-state neutrino interactions individually.

GENIE and NuWro generators are used in this study to simulate the pion generation in neutrino-nucleus interactions. Pions are a common backdrop [9] in so many oscillation studies and their processes in FSI [10] make them theoretically problematic. The DUNE flux has been used for interactions on the ^{40}Ar target in both GENIE and NuWro. Only the CC interactions were analyzed for each generator. Quasi-elastic (QE) scattering, deep-inelastic scattering (DIS), resonance (RES) production, and coherent (COH) pion generation were enabled processes. After that, the data were examined for different pion topologies before (primary interactions) and after final-state interactions (secondary interactions). Understanding the neutrino-nucleus interactions is critical for current experiments like T2K [11] and NOvA [12], as well as upcoming long-baseline neutrino-oscillation experiments like DUNE [13–15] and Hyper–KamioKande [16].

The Deep Underground Neutrino Experiment (DUNE) is a global initiative to build a long-baseline neutrino oscillation experiment at the Fermi National Accelerator Laboratory (FNAL) in the United States. It has a Near Detector (ND) located 575 m from the neutrino source and 60 m underground [17] at Fermilab in Illinois and a Far Detector (FD) located approximately 1.5 km underground at Sanford Underground Research Facility (SURF) in South Dakota, is nearly 1300 km away from Fermilab. The primary scientific goals of this cutting-edge detector are to conduct a thorough programme of neutrino oscillation observations using Fermilab's ν_μ and $\bar{\nu}_\mu$ beams, as well as to restrict the CP violation phase in the leptonic sector. Because the distance between FD and ND is approximately 1300 km, it will give a 1300-km baseline facility for studying the matter effect. Both ND and FD will observe the neutrino spectrum with the Ar target material, which will enable one to overcome numerous systematic uncertainties. The unoscillated neutrino spectrum will be observed by ND, whereas the oscillated neutrino spectrum will be observed by FD. The proportions and technology of the ND and FD at DUNE will be different. The DUNE Near Detector is made up of three basic detector components, two of which can travel off the beam axis: 1) A 50-ton LArTPC (ND-LAr) with pixellated readout built with ArgonCube. 2) The ND-GAr detector, which consists of a high-pressure gaseous argon TPC enclosed by an electromagnetic calorimeter (ECAL) in a 0.5 T magnetic field. 3) The System for on-Axis Neutrino Detection (SAND), an on-axis beam monitor that tracks the neutrino flux. It comprises of a huge solenoidal magnet with an inner tracker surrounding an ECAL. In the current scenario, two inner tracker methods are considered: one using a mix of plastic scintillator cubes and TPCs, and the other using straw tubes.

The DUNE neutrino flux [18] in the range of energies 0.125–10 GeV was employed in our simulation. Figure 1 depicts the ν_μ and $\bar{\nu}_\mu$ flux employed

in our simulations. It peaks at about 2.5 GeV and covers the energy range from a few hundred MeV to tens of GeV. The Neutrinos at Main Injector (NuMI) beamline facility at Fermilab produce the high-purity intense wide-band neutrino beam with an initial output of 1.2 MW (which will be expanded to 2.4 MW) that is estimated to produce 1.1×10^{21} protons each year. The primary beam of protons from the main injector accelerator, with energies ranging from 60 to 120 GeV, collides with the graphite target, producing pions and kaons. With the help of magnetic horns, these mesons will be focused even further toward a 200-m-long decay pipe, in which they will break into neutrinos and leptons. By reversing the polarity of focussing magnets, the neutrino, and antineutrino beams can be expelled individually.

The portions of this paper are as follows: The pion generation in neutrino-nucleus interactions is described in Section 2. The processes of QE, RES, DIS, and COH are explained in depth in this section as well. Section 3 provides an overview of the GENIE and NuWro MC generators, as well as the numerous models that they employ. The simulation results are presented in Section 4, followed by a summary and conclusions in Section 5.

2. Pion Production in Neutrino-Nucleus Interactions

The most basic account of neutrino-nucleus interactions consists of a description of neutrino-nucleus scattering and a framework for nucleons in the nucleus. The simulation of neutrino-nucleus interactions is complicated due to the need to combine many different ideas. We will focus on neutrino-nucleus interactions in the nuclear context. The generator-specific hadronization process explanations and final-state interaction models are common.

In its simplest and most popular form (known as the impulse approximation technique), the neutrino-nucleus scattering is defined as the incoherent sum of scatterings from unbound nucleons in the nucleus. However, because nucleons in the nucleus are in bound states rather than independent particles, finding the cross-section necessitates a more complex understanding of the nuclear dynamics. Charged-current neutrino-nucleus scattering has a total cross-section [19]:

$$\sigma_{\nu N}^{\text{tot}} = \sigma_{\nu N}^{\text{QE}} + \sigma_{\nu N}^{1\pi} + \sigma_{\nu N}^{2\pi} + ... \sigma_{\nu N}^{1K} ... + \sigma_{\nu N}^{\text{DIS}}. \quad (1)$$

Here, ν refers to a neutrino, N refers to a nucleon, $\sigma_{\nu N}^{\text{tot}}$ refers to the sum of all cross-sections, $\sigma_{\nu N}^{\text{QE}}$ refers to the cross-section for QE scattering, $\sigma_{\nu N}^{1\pi}$ refers to the cross-section for the single pion generation, and so on.

Neutrinos interact with matter through the exchange of $W^{\pm}$ and Z^0 bosons. At low neutrino energies, the QE scattering process is favored. As the neutrino energy rises, RES and then DIS processes become more important as seen in Fig. 2 for both neutrino and antineutrino. Around 2.5 GeV, the DUNE flux peaks and the RES and DIS cross-sections are nearly similar at this energy. RES events can have signals that are indistinguishable from DIS events in a detector, which is a problem in practice. As a result, it is difficult to measure each stage separately.

In the QE scattering, the target nucleon remains a single nucleon in the final state, only changing its charge in CC weak interactions. This scattering does not make pions directly, but it can produce them through final-state interactions. Inside the nuclear environment, hadrons can be spread elastically or inelastically, absorbed or charge-exchanged, and even produce more pions. As a result, only a small percentage of events with no pions in the primary state is expected to produce pions in the final state. For the ν_μ beam, the CC QE scattering reaction is written as:

$$\nu_\mu + n \longrightarrow \mu^- + p. \quad (2)$$

Figure 3 illustrates how pions are produced in the QE scattering process (left) and how a pion could be absorbed (right) inside the nucleus during its intranuclear journey. The most prevalent processes that directly produce pions are DIS, RES, and COH. These processes are depicted in Fig. 4.

In the RES scattering, resonances produce ions. In the RES production process, a neutrino excites the target nucleon to a resonance state. The resonance state that is formed quickly decays into a single nucleon and pion state. The $\Delta(1232)$ resonance state contributes the most to this process, but higher resonance levels can also be generated. The CCRES scattering processes (for ν_μ beam) are as follows:

$$\nu_\mu + p \longrightarrow \mu^- + \Delta^{++};\ \Delta^{++} \longrightarrow p + \pi^+, \quad (3)$$

$$\nu_\mu + n \longrightarrow \mu^- + \Delta^{+};\ \Delta^{+} \longrightarrow n + \pi^+, \quad (4)$$

$$\nu_\mu + n \longrightarrow \mu^- + \Delta^{+};\ \Delta^{+} \longrightarrow p + \pi^0. \quad (5)$$

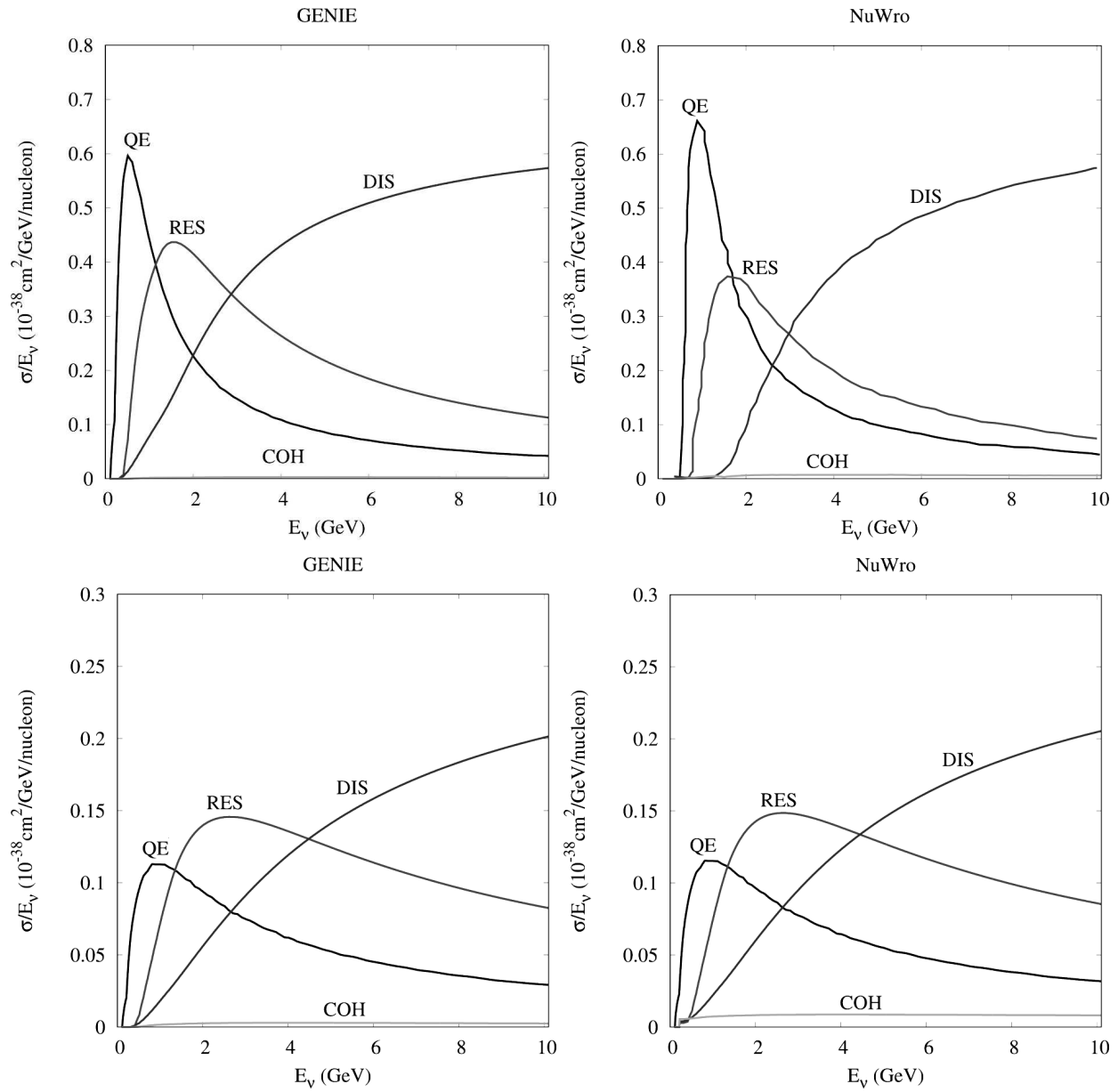

Fig. 2. ν_μ-Ar (top panel) and $\bar{\nu}_\mu$-Ar (bottom panel) interaction cross-section per nucleon as a function of the neutrino energy by GENIE (left panel) and NuWro (right panel) in the energy regime 1–10 GeV, for different charged current processes considered in our work

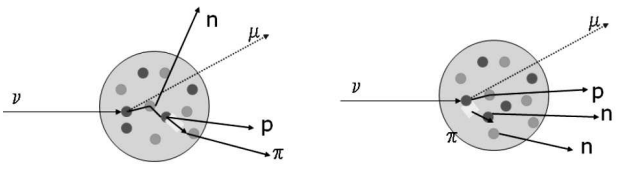

Fig. 3. Pion production in the QE scattering (left) and absorption in the RES scattering (right) [2]

When a pion created in a RES process is absorbed in the nucleus, establishing whether the process is RES becomes difficult. As a result, the staged event is referred to as a fake event, because it gives the appearance of a separate procedure. The particles recorded by the detector are like those formed at the primary vertex in a specific interaction channel.

A high-energy neutrino penetrates deep into the nucleon and scatters off a quark via the exchange of $W^{\pm}$ and Z^0 bosons, resulting in a lepton and a hadronic system in the ultimate state of DIS. The CC ν_μ interaction process is as follows:

$$\nu_\mu + N \longrightarrow \mu^- + n\pi^{\pm} + X, \tag{6}$$

where N is a nucleon (proton or neutron), n denotes a number, and X denotes any group of final nucleons.

Neutrinos can interact coherently with the entire nucleus, resulting in the pion generation (coherent (COH) pion production). The approach for the CC ν_μ interaction is as follows:

$$\nu_\mu + A \longrightarrow \mu^- + A' + m^+, \tag{7}$$

where A is the nucleus in its initial state, A' is the nucleus in its final state, and $m^+ = \pi^+$, k^+, $\rho^+ \ldots$.

3. Event Generators

Neutrino event generators are simulation tools used in neutrino physics researches, and they can be improved utilizing experimental data from previous studies. Generators serve as a link between theoretical and experimental frameworks. GENIE (Generates Events for Neutrino Interaction Experiments) and NuWro are the two neutrino event generators employed in this study (developed at Wroclaw University). In our simulations, we employed GENIE version 3.00.06 and NuWro version 19.01, which are the most recent stable releases.

3.1. Genie

Cross-section models, hadronization models, and nuclear physics models are the three types of physics models employed in GENIE. Charged-current quasielastic scattering is described for cross-sections using the Llewellyn–Smith model [21] and the newest BBBA07 form factors [22]. The Rein–Sehgal model [23] was used to generate baryon resonances. The Bodek and Yang model [24] is utilized for DIS interactions, with low Q^2 modifications. For the coherent pion production interactions, the Rein–Sehgal model with an updated PCAC formula [25] is utilized. The default AGKY model is used in the hadronization procedure [26]. It provides a phenomenological description of the low invariant mass region using Koba–Nielson–Olsen (KNO) scaling [27], before progressively switching to the PYTHIA/JETSET model at higher masses, with the transition being gradual and

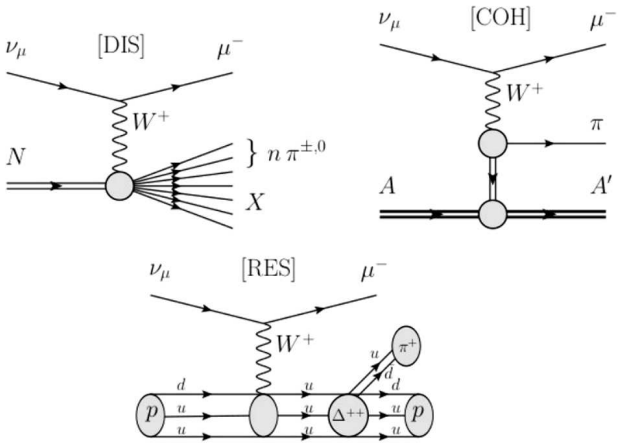

Fig. 4. Pion production via various processes [20]

continuous. To account for the effect of the nuclear environment, the Fermi Gas model is employed, with modifications by Bodek and Ritchie to add nucleon-nucleon interactions. Factors such as the Pauli blocking and discrepancies in free nucleon and nuclear structural functions are also taken into account. Intranuclear hadron transport is handled by the INTRANUCLEAR/hA model.

3.2. NuWro

QE events are simulated in NuWro using the Llewellyn–Smith model with the most recent BBBA05 form factors [28]. Only the $\Delta(1232)$ contribution is based on the Rein–Sehgal model in RES, whereas the remainder of the resonances are based on the Adler–Rarita–Schwinger model [29]. The simulation of coherent pion production interactions is done using the Rein–Sehgal model. This Rein–Sehgal model [25] is not the same as the one used in RES. A cut on invariant mass of $W < 1.4$ GeV defines the RES zone. NuWro describes DIS events using the Quark–Parton model [30]. When $W > 1.6$ GeV, the DIS contribution is enabled. The RES contribution is linearly turned off, as the DIS contribution is turned on in the area 1.4 GeV $< W <$ 1.6 GeV. NuWro employs a combination of its hadronization model and the Bodek–Yang model. The Relativistic Fermi Gas (RFG) model is used to account for the impacts of the nuclear environment.

4. Results

We have generated 1 million similar sets of events for both ν_μ and $\bar{\nu}_\mu$ GENIE and NuWro. For each gen-

Table 1. **Occupancy of primary and final-state hadronic systems for 1 million events in GENIE(v3.00.06) for ν_μ-Ar CC interactions. Different topological groups for primary and final-state systems were made on the basis of the number of pions produced eventwise**

Final State	Primary hadronic system											Total
	0π	π^0	π^+	π^-	$2\pi^0$	$2\pi^+$	$2\pi^-$	$\pi^0\pi^+$	$\pi^0\pi^-$	$\pi^+\pi^-$	$\geq 3\pi$	
0π	**243 896**	24 393	76 207	237	180	485	0	1 423	25	354	375	347 577
π^0	2 652	**77 505**	45 010	188	2 049	516	0	6 959	49	337	1 353	136 618
π^+	4 098	7 742	**222 782**	215	75	3 275	0	6 424	6	1 915	1 488	248 020
π^-	739	7 375	2 881	**639**	85	9	0	412	31	1 903	610	14 684
$2\pi^0$	3	3 102	6 912	71	**5 545**	215	0	3 295	27	181	2 251	21 602
$2\pi^+$	10	419	3 330	7	11	**7 829**	0	1 443	1	50	1 917	15 017
$2\pi^-$	0	93	17	5	16	0	**0**	4	5	11	88	239
$\pi^0\pi^+$	42	5 600	11 622	155	531	1 739	0	**32 756**	2	1 026	4 331	57 802
$\pi^0\pi^-$	13	2 969	1 896	135	684	18	0	456	**121**	1 055	1 525	8 872
$\pi^+\pi^-$	32	10 013	31 548	681	241	404	0	3 290	15	**12 070**	3 585	61 879
$\geq 3\pi$	95	3 350	6 095	497	1 836	2 295	0	9 956	240	4 066	**59 260**	87 690
Total	251 582	142 561	408 300	2 830	11 253	16 785	0	66 418	520	22 968	76 783	1 000 000

Table 2. **Occupancy of primary and final-state hadronic systems for 1 million events in GENIE(v3.00.06) for $\bar{\nu}_\mu$-Ar CC interactions. Different topological groups for primary and final-state systems were made based on the number of pions produced eventwise**

Final State	Primary hadronic system											Total
	0π	π^0	π^+	π^-	$2\pi^0$	$2\pi^+$	$2\pi^-$	$\pi^0\pi^+$	$\pi^0\pi^-$	$\pi^+\pi^-$	$\geq 3\pi$	
0π	**280 968**	23 903	212	94 301	161	0	309	4	1 058	359	269	401 544
π^0	1 376	**62 882**	190	55 269	1 318	0	282	21	5 304	370	948	127 960
π^+	330	5 932	**441**	904	73	0	6	14	225	1 390	419	9 734
π^-	2 707	9 650	244	**240 693**	121	0	2 603	1	4 824	1 371	1 041	263 255
$2\pi^0$	4	2 810	69	5 339	**3 147**	0	132	9	2 442	176	1 551	15 679
$2\pi^+$	0	44	1	7	10	**0**	0	1	0	4	48	115
$2\pi^-$	18	664	5	3 661	15	0	**7 407**	0	1 412	58	1 786	15 026
$\pi^0\pi^+$	4	1 831	138	512	314	0	9	**45**	265	704	925	4 747
$\pi^0\pi^-$	34	6 261	199	8 822	437	0	1 484	7	**24 415**	709	3 676	46 044
$\pi^+\pi^-$	24	7 644	744	21 456	167	0	309	3	2 036	**7 146**	2 855	42 384
$\geq 3\pi$	144	2 821	364	3 559	1 093	0	2 684	157	9 130	2 816	**50 744**	73 512
Total	285 609	124 442	2 607	434 523	6 856	0	15 225	262	51 111	15 103	64 262	1 000 000

erator, the number of pions created in both primary and final states was determined event by event. These simulated results are displayed in tables that indicate the topologies of pion formed in the primary and final states. The topology of the pions created in primary neutrino-nucleus interactions is stored in a primary state. A final state contains the topology of the pions produced after any secondary interactions (such as the intra-atomic scattering or absorption) have occurred. A description of the generators' models and physics choices has previously been provided for a fair comparison of generators.

Table 1 shows the results of GENIE simulations for 1 million ν_μ events and Table 2 for 1 million $\bar{\nu}_\mu$ events using default axial mass parameters of $M_A^{\mathrm{QE}} = 0.99$ GeV/c^2 and $M_A^{\mathrm{RES}} = 1.12$ GeV/c^2. The

Table 3. **Occupancy of primary and final-state hadronic systems for 1 Million events in NuWro(v19.01.2) for ν_μ-Ar CC interactions. Different topological groups for primary and final state systems were made on the basis of number of pions produced event-wise**

Final State	Primary hadronic system											Total
	0π	π^0	π^+	π^-	$2\pi^0$	$2\pi^+$	$2\pi^-$	$\pi^0\pi^+$	$\pi^0\pi^-$	$\pi^+\pi^-$	$\geq 3\pi$	
0π	**242 200**	16 748	55 659	622	141	133	0	1 533	10	759	66	317 871
π^0	3 596	**84 684**	14 875	136	1 720	94	0	10 810	122	486	774	117 297
π^+	5 790	3 748	**210 329**	21	51	1 722	0	9 958	3	5 169	516	237 307
π^-	2 454	4 361	3 172	**6 581**	69	14	1	479	92	5 475	397	23 095
$2\pi^0$	483	1 823	966	7	**6 785**	17	0	3 365	24	113	2 520	16 103
$2\pi^+$	94	120	2 354	0	4	**6 095**	0	2 073	1	333	1 206	12 280
$2\pi^-$	58	122	108	31	11	1	**2**	35	20	351	124	863
$\pi^0\pi^+$	350	1 974	4 311	3	396	502	0	**80 723**	5	1 810	4 720	94 794
$\pi^0\pi^-$	249	1 360	780	50	426	8	0	967	**1 126**	1 769	2 956	9 691
$\pi^+\pi^-$	389	1 269	4 920	86	31	113	0	2 942	23	**45 126**	4 659	59 558
$\geq 3\pi$	223	1 577	2 865	24	687	495	0	8 600	69	4 546	**92 055**	111 141
Total	255 886	117 786	300 339	7 561	10 321	9 194	3	121 485	1 495	65 937	109 993	1 000 000

Table 4. **Occupancy of primary and final-state hadronic systems for 1 Million events in NuWro(v19.01.2) for $\bar{\nu}_\mu$-Ar CC interactions. Different topological groups for primary and final state systems were made on the basis of number of pions produced event-wise**

Final State	Primary hadronic system											Total
	0π	π^0	π^+	π^-	$2\pi^0$	$2\pi^+$	$2\pi^-$	$\pi^0\pi^+$	$\pi^0\pi^-$	$\pi^+\pi^-$	$\geq 3\pi$	
0π	**296 715**	16 914	71	75 785	186	0	224	1	1 818	777	68	392 559
π^0	2 073	**59 145**	22	17 674	1 807	0	100	11	10 292	404	512	92 040
π^+	1 060	2 960	**578**	2 324	81	0	19	13	423	3 675	233	11 366
π^-	5 312	4 370	6	**259 892**	104	0	2 419	0	10 815	4 111	498	287 527
$2\pi^0$	259	1 081	1	795	**5 722**	0	12	1	2 712	75	1 840	12 498
$2\pi^+$	8	50	2	38	5	**0**	0	0	20	146	46	315
$2\pi^-$	64	158	0	2 986	15	0	**8 426**	0	2 764	311	1 305	16 029
$\pi^0\pi^+$	57	655	6	433	313	0	7	**85**	553	1 026	1 658	4 793
$\pi^0\pi^-$	198	1 651	1	4 381	506	0	619	2	**66 307**	1 272	3 665	78 602
$\pi^+\pi^-$	187	849	11	3 355	34	0	107	1	2 262	**26 842**	3 018	36 666
$\geq 3\pi$	86	641	3	1 599	494	0	564	7	5 547	2 131	**56 533**	67 605
Total	306 019	88 474	701	369 262	9 267	0	12 497	121	103 513	40 770	69 376	1 000 000

occupancy of the primary and final-state topologies is shown in the tables. Figure 5 shows a comparative plot for primary and final-state pions in GENIE (left panel) for ν_μ (top left panel) and $\bar{\nu}_\mu$ (bottom left panel).

Table 3 shows the results of NuWro simulations for 1 million ν_μ events and Table 4 for 1 million $\bar{\nu}_\mu$ events using default axial mass parameters of $M_A^{\mathrm{QE}} = 1.03$ GeV/c^2 and $M_A^{\mathrm{RES}} = 0.94$ GeV/c^2. The occupancy of the primary and final-state topologies is shown in the tables. Figure 5 shows a comparative plot for primary and final-state pions in NuWro (right panel) for ν_μ (top right panel) and $\bar{\nu}_\mu$ (bottom right panel).

In the case of ν_μ, Tables 1 (GENIE) and 3 (NuWro) illustrate that, for two generators, there are con-

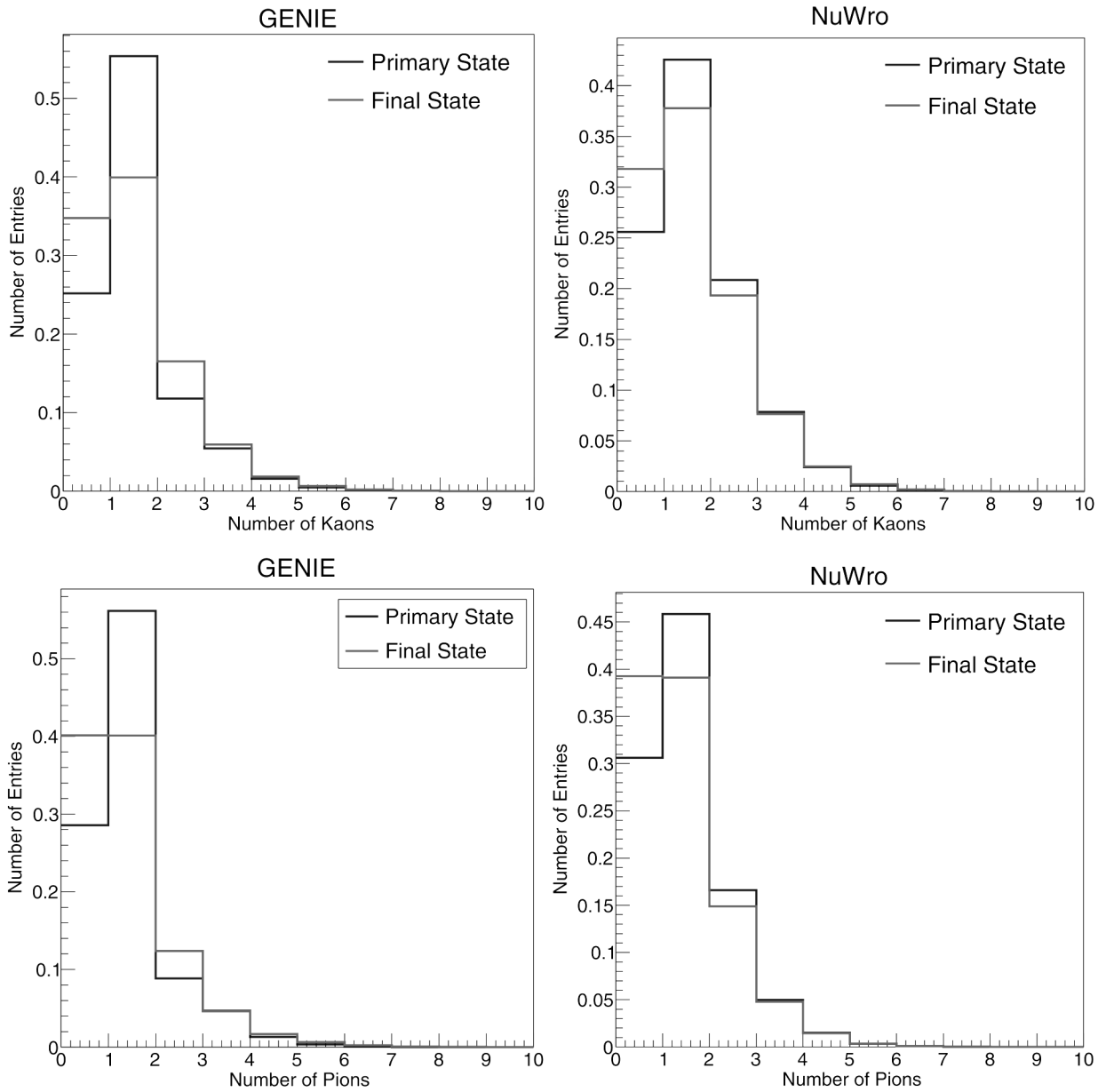

Fig. 5. Number of pions produced on event by event basis in primary and final states for GENIE (left panel) and NuWro (right panel) generators. Blue lines represent primary states and red lines represent final states in both the panels

siderable differences in both primary and final-state topologies (i.e., the number of pions seen in the primary and final states). Figure 5 (top panel) provides plots for each generator's number of pions observed on an event-by-event basis in the main and final states, revealing the disparities. Frequently, these differences are higher than statistical fluctuations. The number of π^+ observed in the final state corresponding to π^0 in the primary state for GENIE is 7742, but the number for NuWro is 3748, a difference of more than 50%. The number of π^0 observed in the final state matching π^+ in the primary state for GENIE is 45010, but the figure for NuWro is 14875, which is a significant difference. The number of π^-

observed in the final state equivalent π^- in the primary stage for GENIE is 639, whereas the figure for NuWro is 6581. The reason for these discrepancies is that DUNE flux peaks near 2.5 GeV, but QE, RES, and DIS processes all contribute significantly to the overall cross-section in this energy region. Although the models used to explain these processes are commonly shared among generators, there are numerous differences in how each generator views the merging of relative impact in this energy zone. When this effect is paired with other input parameters, visible differences across models can emerge.

In the case of $\bar{\nu}_\mu$, Tables 2 (GENIE) and 4 (NuWro) illustrate that, for two generators, there are considerable differences in both primary and final-state topologies (i.e., the number of pions seen in primary and final states). Figure 5 (bottom panel) provides plots for each generator's number of pions observed on an event-by-event basis in the main and final states, revealing the disparities. The number of π^+ observed in the final state corresponding to π^0 in the primary state for GENIE is 5932, but the number for NuWro is 2960, a difference of more than 50%. The number of π^0 observed in the final state matching π^- in the primary state for GENIE is 55269, but the figure for NuWro is 17674, which is a significant difference.

The final states of both generators have a higher number of zero pion (0π) topologies than the primary states, according to the tables in both the cases. This means that pions can be absorbed more easily than they can be created through the intranuclear transit. Topologies with pions in the primary and final states are more likely to be produced by RES and DIS processes, whereas topologies with 0π in the primary and final states are more likely to be produced by QE processes. Furthermore, the generators' topologies are almost identical. Changes in nuclear models and form factors utilized in each generator could explain the differences.

Using Tables 1 and 3 for ν_μ and Tables 2 and 4 for $\bar{\nu}_\mu$ illustrates the fraction of events with no pion (0π), exactly one pion (1π), and more than one pion ($> 1\pi$). Single pion production (1π), however, is recommended in GENIE, whereas multiple pion production is preferred in NuWro.

Using Tables 1 and 3, Table 5 illustrates the fraction of events with no pion (0π), exactly one pion (1π), and more than one pion ($> 1\pi$) in the case of ν_μ. Using Tables 2 and 4, Table 6 illustrates the fraction of events with no pion (0π), exactly one pion (1π), and more than one pion ($> 1\pi$) in the case of ν_μ. Single pion production (1π), however, is recommended in GENIE, whereas multiple pion production is preferred in NuWro.

Tables 1, 2, 3, and 4 reveal the important information about final-state interactions. To collect this data, we produced a summary table (Table 7 for ν_μ

Table 5. **Percentage of events without pion (0π), with exactly one pion (1π) and with more than one pion ($>1\pi$) for ν_μ-Ar CC interactions. Values in brackets refer to results after final-state interactions**

Pions	GENIE, %	NuWro, %
0π	25.2 (34.8)	25.6 (31.8)
$1\pi^0$	14.2 (13.7)	11.8 (11.7)
$1\pi^+$	40.8 (24.8)	30 (23.7)
$1\pi^-$	0.3 (1.5)	0.8 (2.3)
1π	55.3 (39.9)	42.6 (37.7)
$>1\pi$	19.5 (25.3)	31.8 (30.5)

Table 6. **Percentage of events without pion (0π), with exactly one pion (1π) and with more than one pion ($1 > \pi$) for $\bar{\nu}_\mu$-Ar CC interactions. Values in brackets refer to results after final state interactions**

Pions	GENIE, %	NuWro, %
0π	28.6 (40.1)	30.6 (39.3)
$1\pi^0$	12.4 (12.8)	8.8 (9.2)
$1\pi^+$	0.3 (1.0)	0.1 (1.1)
$1\pi^-$	43.4 (26.3)	36.9 (28.9)
1π	56.1 (40.1)	45.8 (39.1)
$>1\pi$	15.3 (19.8)	23.6 (21.5)

Table 7. **Percentage of events with single pion or no pion in the final state, if there was a single pion in the primary state for ν_μ-Ar CC interactions**

Pions	GENIE, %	NuWro, %
$\pi^0 \to \pi^0$	54.4	71.9
$\pi^+ \to \pi^+$	54.6	70
$\pi^0 \to 0\pi's$	17.1	14.2
$\pi^+ \to 0\pi's$	18.7	18.5
$\pi^0 \to \pi^+$	5.4	3.2
$\pi^0 \to \pi^-$	5.2	3.7
$\pi^+ \to \pi^0$	11	5

Table 8. **Percentage of events with single pion or no pion in the final state, if there was a single pion in the primary state for $\bar{\nu}_\mu$-Ar CC interactions**

Pions	GENIE, %	NuWro, %
$\pi^0 \to \pi^0$	50.5	66.9
$\pi^- \to \pi^-$	55.4	70.4
$\pi^0 \to 0\pi's$	19.2	19.1
$\pi^- \to 0\pi's$	21.7	20.5
$\pi^0 \to \pi^+$	4.8	3.3
$\pi^0 \to \pi^-$	5.2	4.9
$\pi^- \to \pi^0$	12.7	20.5

and Table 8 for $\bar{\nu}_\mu$). The summary table depicts the topology-changing effect of intranuclear hadron transit. Out of all events having a certain primary state topology, we present the fraction of occurrences with both primary and final-state topologies for each generator in this table. In the first two rows, the nucleus is translucent. These rows represent the percentage of occurrences with 1π in the primary state that will still have 1π in the final state. The pion formed in the primary vertex is more likely to not re-interact, as we can see. The effect of charge exchange is shown in the next three rows, while the fraction of pions absorbed is shown in the following rows. NuWro's current version (v19.01) is significantly more transparent than GENIE's current version (v3.00.06). This could be due to a generator's sensitivity to the absorption and charge exchange processes (NuWro may have too little, whereas GENIE may have too much). Despite these differences, given the complicated nature of final-state interactions, one could argue that the agreement is still good. The results of the analyzed MC generators are very similar. The finding could be particularly useful because single pion events make up the majority of the background in neutrino oscillation investigations.

5. Summary and Conclusions

In this paper, we look at the effect of final-state contacts on pion production for $\nu_\mu(\bar{\nu}_\mu)$ -nucleus interactions on a ^{40}Ar target in detail. The most recent versions of the GENIE and NuWro generators were used as simulation tools. Despite having comparable sets of models, two generators can have differing pion production results in the primary and final states, as seen in Tables 1, 2, 3, and 4. This could be because the two generators implement models and other input parameters differently. Both generators show essentially equal impacts of final-state interactions on pions during their intranuclear trip after being produced at the primary vertex. This is seen in Tables 5 and 6. As demonstrated in Fig. 5, final-state interactions cause a difference between pions observed in the detector (final-state pions) and pions created at the primary vertex (pions in the primary state). In addition, Tables 1, 2, 3, and 4 reveal that both generators have more 0π topologies in the final state than in the primary state, meaning that pions are more likely to be absorbed than formed during their intranuclear transit.

Our findings suggest that the ideal method for a neutrino oscillation experiment like DUNE is to have authentic correctness of nuclear models used in neutrino event generators employed for the simulation, which necessitate the use of a canonical neutrino event generator. Understanding nuclear consequences necessitates a thorough understanding of hadronic physics of neutrino-nucleus interactions.

One of the authors, Miss Ritu Devi offers most sincere gratitude to the Council of Scientific and Industrial Research (CSIR), Government of India, for the financial support in the form of Senior Research Fellowship, file No. 09/100(0205)/2018-EMR-I.

1. C. Giganti, S. Lavignac, M. Zito. Neutrino oscillations: the rise of the PMNS paradigm. *Prog. Part. Nucl. Phys.* **98**, 1 (2018).
2. C. Andreopoulos, C. Barry, S. Dytman, H. Gallagher, T. Golan, R. Hatcher, G. Perdue, J. Yarba. The GENIE neutrino Monte Carlo generator: Physics and user manual. arXiv:1510.05494 (2015).
3. A. Gazizov, M.P. Kowalski. ANIS: High energy neutrino generator for neutrino telescopes. *Comput. Phys. Commun.* **172**, 203 (2005).
4. T. Golan, C. Juszczak, J.T. Sobczyk. Effects of final-state interactions in neutrino-nucleus interactions. *Phys. Rev. C* **86**, 015505 (2012).
5. O. Buss, T. Gaitanos, K. Gallmeister, H. van Hees, M. Kaskulov, O. Lalakulich, A.B. Larionov, T. Leitner, J. Weil, U. Mosel. Transport-theoretical description of nuclear reactions. *Phys. Rept.* **512**, 1 (2012).
6. S. Gardiner. Simulating low-energy neutrino interactions with MARLEY. *Comput. Phys. Commun.* **269**, 108123 (2021).
7. Y. Hayato. NEUT. *Nucl. Phys. B Proc. Suppl.* **112**, 171 (2002).
8. D. Casper. The nuance neutrino physics simulation, and the future. *Nucl. Phys. B Proc. Suppl.* **112**, 161 (2002).

9. P. Abratenko *et al.* (MicroBooNE Collaboration). Search for an anomalous excess of charged-current ν_e interactions without pions in the final state with the MicroBooNE experiment. arXiv:2110.14065 [hep-ex] (2021).
10. S. Naaz, A. Yadav, J. Singh, R. B. Singh. Effect of final state interactions on neutrino energy reconstruction at DUNE. *Nucl. Phys. B* **933**, 40 (2018).
11. K. Abe *et al.* (T2K Collaboration). Constraint on the matter–antimatter symmetry-violating phase in neutrino oscillations. *Nature* **580**, 7803 (2020).
12. M.A. Acero *et al.* (NOvA Collaboration). First measurement of neutrino oscillation parameters using neutrinos and antineutrinos by NOvA. *Phys. Rev. Lett.* **123**, 151803 (2019).
13. B. Abi *et al.* (DUNE Collaboration). Deep underground neutrino experiment (DUNE), far detector technical design report, Volume I introduction to DUNE. *JINST* **15**, 08, T08008 (2020).
14. B. Abi *et al.* (DUNE Collaboration). Deep underground neutrino experiment (DUNE), far detector technical design report, Volume II DUNE Physics, arXiv:2002.03005 [hep-ex] (2020).
15. B. Abi *et al.* (DUNE Collaboration). Experiment simulation configurations approximating DUNE TDR. arXiv:2103.04797 [hep-ex] (2021).
16. K. Abe *et al.* (Hyper-Kamiokande Collaboration) Hyperkamiokande design report. arXiv: 1805.04163 [physics.ins-det] (2018).
17. B. Abi *et al.* (DUNE collaboration). Long-baseline neutrino oscillation physics potential of the DUNE experiment. *Eur. Phys. J. C* **80**, 978 (2020).
18. http://home.fnal.gov/ ljf26/DUNE2015CDRFluxes /NuMI_Improved_80GV_StandardDP /g4lbne_v3r2p4b_FHC_ND_globes_flux.txt.
19. K.S. Kuzmin, V.V. Lyubushkin, V.A. Naumov. How to sum contributions into the total charged-current neutrino-nucleon cross section. arxiv:0511308 [hep-ph] (2005).
20. M. Antonello, V. Caracciolo, G. Christodoulou, J. Dobson, E. Frank, T. Golan, V. Lee, S. Mania, P. Przewlocki, B. Rossi, D. Stefan, R. Sulej, T. Szeglowski, R. Tacik, T. Wachala. Study of pion production in ν_μ CC interactions on O^{16} using different MC generators. *Acta Phys. Polon. B* **40**, 2519 (2009).
21. C.H. Llewellyn Smith. Neutrino reactions at accelerator energies. *Phys. Rept.* **3**, 261 (1972).
22. A. Bodek, S. Avvakumov, R. Bradford, H. Budd. Modeling atmospheric neutrino interactions: Duality constrained parameterization of vector and axial nucleon form factors. In: *30th International Cosmic Ray Conference.* arxiv:0708.1827 (2007).
23. D. Rein, L.M. Sehgal. Neutrino excitation of baryon resonances and single pion production. *Ann. Phys.* **133**, 79 (1981).
24. A. Bodek, U.K. Yang. Higher twist, xi(omega) scaling, and effective LO PDFs for lepton scattering in the few GeV region. *J. Phys. G* **29**, 1899 (2003).
25. D. Rein, L.M. Sehgal. Coherent π^0 production in neutrino reactions. *Nucl. Phys. B* **223**, 29 (1983).
26. J. Tena-Vidal, C. Andreopoulos, C. Barry, S. Dennis, S. Dytman, H. Gallagher, S. Gardiner, W. Giele, R. Hatcher, O. Hen, I.D. Kakorin, K.S. Kuzmin, A. Meregaglia, V.A. Naumov, A. Papadopoulou, M. Roda, V. Syrotenko, J. Wolcott. Hadronization model tuning in genie v3. *Phys. Rev. D* **105**, 012009 (2022).
27. Z. Koba, H.B. Nielsen, P. Olesen. Scaling of multiplicity distributions in high-energy hadron collisions. *Nucl. Phys. B* **40**, 317 (1972).
28. R. Bradford, A. Bodek, H. Budd, J. Arrington. A new parameterization of the nucleon elastic form-factors. *Nucl. Phys. B Proc. Suppl.* **159**, 127 (2006).
29. K.M. Graczyk, D. Kielczewska, P. Przewlocki, J.T. Sobczyk. C_5^A axial form factor from bubble chamber experiments *Phys. Rev. D* **80**, 093001 (2009).
30. T. Sjostrand, S. Mrenna, P.Z. Skands. PYTHIA 6.4 Physics and Manual *JHEP* **05**, 026 (2006).

Received 26.05.22

Р. Деві, Б. Потукучі

ГЕНЕРАЦІЯ ПІОНІВ У ВЗАЄМОДІЇ ν_μ ІЗ ЗАРЯДЖЕНИМ СТРУМОМ НА ^{40}Ar В ЕКСПЕРИМЕНТАХ ІЗ НЕЙТРИНО ГЛИБОКО ПІД ЗЕМНОЮ ПОВЕРХНЕЮ

Аналіз процесу генерації піонів і наслідків взаємодії в кінцевому стані (ВКС) є критично важливим для обробки даних у всіх нейтринних експериментах. Енергія, яка використовується у сучасних дослідженнях процесів резонансної генерації нейтрино, дає значний внесок у народження піонів. Якщо піон після його народження поглинається ядерною речовиною, цю подію можна не відрізнити від квазіпружного розсіяння і віднести до фону. Для експериментів з осциляціями нейтрино оцінка цього фону є критично важливою, що вимагає надійних теоретичних моделей як для генерації піонів у первинній вершині, так і після ВКС. Кількість піонів, утворених після ВКС, значно відрізняється від тієї кількості, яка народжується у первинній вершині. Оскільки детектори нейтрино можуть виявляти лише частинки в кінцевому стані, то ефекти ВКС приховують правильну інформацію про частинки, утворені в первинній вершині. Для розв'язання цієї проблеми потрібно детальне дослідження ВКС, яке можна реалізувати в рамках теоретичних моделей, включених в генератори нейтринних подій в рамках методу Монте-Карло. В даній роботі виконано моделювання подій з генерацією піона завдяки взаємодії ν_μ із зарядженим струмом на мішені ^{40}Ar в установці DUNE в експериментах з нейтрино глибоко під земною поверхнею з використанням двох програм: GENIE та NuWro. У порівнянні з GENIE (v-3.00.06), програма NuWro (v-19.02.2) є менш придатною для опису процесів обміну зарядом і поглинання. Піони скоріше поглинаються, ніж утворюються під час руху всередині ядра.

Ключові слова: взаємодія у кінцевому стані, поперечний переріз, нейтрино-ядерне розсіювання, первинна адронна система.